Title
FURTHER THEORETICAL RESULTS ON THE STABILITY OF SUPER-HEAVY NUCLEI

Authors
Tsang, Chin Pu
Nilsson, Sven Gosta.

Publication Date
1969-08-01

Submitted to Nuclear Physics

UCRL-18966
Preprint

FURTHER THEORETICAL RESULTS ON THE STABILITY OF SUPERHEAVY NUCLEI

Chin Fu Tsang and Sven Gösta Nilsson

August 1969

AEC Contract No. W-7405-eng-48

LAWRENCE RADIATION LABORATORY
UNIVERSITY of CALIFORNIA BERKELEY

UCRL-18966

DISCLAIMER

UCRL-18966

FURTHER THEORETICAL RESULTS ON THE STABILITY OF SUPERHEAVY NUCLEI[†]

Chin Fu Tsang and Sven Gösta Nilsson[††]

Lawrence Radiation Laboratory
University of California
Berkeley, California 94720

August 1969

Abstract

Theoretical results are exhibited for the stability of superheavy nuclei with $106 \leqslant Z \leqslant 128$ and $176 \leqslant N \leqslant 204$ with respect to various decay mechanisms. A discussion is given of the production of superheavy nuclei by heavy-ion reactions. In particular, the experimental possibilities associated with the ^{86}Kr beam are considered on the basis of the present calculations.

[†]Work performed under the auspices of the U. S. Atomic Energy Commission.

[††]On leave of absence from the Lund Institute of Technology, Lund, Sweden.

1. Introduction

Great interest in the study of superheavy nuclei was initiated by the work of Myers and Swiatecki[1]), who showed that an island of stability against spontaneous fission may be expected around a region of doubly-closed nucleon shells. Various single-particle calculations[2]) suggested Z = 114 and N = 184 as the closest magic numbers beyond the region of known nuclei. The predicted island of stability around $^{298}114_{184}$ is estimated to be centered near the extrapolated beta-stability line and may turn out to be accessible, if not by presently available accelerators and ions, by future experimental techniques.

A recent calculation[3,4]) exhibits the stability of nuclei in this region against spontaneous fission as well as against alpha and beta decays. It leads to the somewhat surprising result that some of these superheavy nuclei might have total half-lives comparable with the age of the solar system.

The shell-structure calculations also indicate a large energy gap in the neutron single-particle energy diagram at N = 196 (for a discussion of the relevance of this subshell number see below). Thus the island of stability is predicted also to include the region associated with the neutron number N = 196, which region is not considered in ref. [4]). In the present work we have thus enlarged our region of interest to that of nuclei with $106 \leqslant Z \leqslant 128$ and $176 \leqslant N \leqslant 204$. Half-lives of spontaneous fission and alpha decay as well as the proton and neutron binding energies are calculated. Stability against beta decay is also investigated.

Ion beams such as ^{64}Ni, ^{86}Kr and ^{132}Xe may become available in accelerators of the near future. With appropriate targets these projectiles

would produce compound nuclei in the region studied. A discussion is given of the possible experiments involving the ^{86}Kr beam making use of the present theoretical results.

2. Method of Calculation

The details of the calculation are described in ref. [4]). A generalised harmonic oscillator potential is employed with distortion coordinates ε and ε_4 representing essentially P_2 and P_4 distortions in shape. In addition to spin-orbit force, a shape correction term proportional to $\ell^2 - \langle \ell^2 \rangle_N$ is also included, where the last term represents the average over a given oscillator shell. The strengths of the terms added to the oscillator potential represent two adjustable parameters for protons and two for neutrons, which are fitted to reproduce optimally the observed level order in the actinide ($A \approx 242$) and the rare earth ($A \approx 165$) regions. A linear A-dependence is assumed for these parameters for extrapolations to the superheavy region ($A \approx 300 - 320$). Pairing energy contributions are calculated on the basis of the single-particle levels obtained. The pairing matrix element G is assumed to be isospin dependent and proportional to the surface area of the nucleus. The usually employed conservation of the volume of equipotential surfaces is complimented by the Strutinsky method of liquid-drop normalisation[5]). This method ensures that on the average the behavior of deformation energy is that given by a charged liquid drop. By employing correction terms in the normalisation function up to the sixth order, the final results are stable with respect to the range parameter employed in the normalisation[4,6]). The liquid-drop parameters are taken, without readjustment, from those of the semi-empirical mass formula of Myers and Swiatecki[7]).

3. Results of Calculations

Basic to all of the calculations presented is the possibility to produce a reliable set of single-particle levels. In figs. 1 and 2 one may compare the level schemes predicted by the modified oscillator model with those obtained on the basis of a Woods-Saxon potential, as given in Rost[8]) (compare also, e.g., with those given by Bolsterli, Fiset and Nix[9]) and Chepurnov[10])). The proton level scheme there obtained is in good agreement with ours (see fig. 1). On the other hand the region of subshells around neutron number N = 184 comes out somewhat different (fig. 2). Thus the $h_{11/2}$ orbital is located relatively lower in our case, and, above this orbital, N = 196 appears as a second subshell gap. Thus while the N = 184 is associated with a larger energy gap in the references quoted, in our case the shell gap is split between the gaps of N = 184 and N = 196. It turns out that the summed energy split across N = 184 and N = 196 is somewhat larger in our case. As can be seen from table II of the investigation by Muzychka[11]), different shell model prescriptions result in a remarkably close agreement in the height of the fission barrier peaks of the nuclei in the vicinity of Z = 114 and N = 184. For N = 196 the effect of the difference in level schemes predicted by the alternative potentials remains to be investigated quantitatively. It appears possible that the difference in barrier heights obtained might be more marked there than in the region investigated by Muzychka.

We have in the present investigation extended our calculations into this more controversial region of extrapolation in spite of the discrepancy in level spacing predicted by the different potentials.

Potential-energy surfaces calculated in our model as a function of ε and ε_4 deformations may be studied for each nucleus. In figs. 3 a-n we exhibit the potential energy of isotopes of Z = 116, 118, 120, 122, 124, 126, and 128 as a function of ε with minimization of energy with respect to ε_4 for each value of ε. This type of plot represents a cut through the two-dimensional energy surface along the potential-energy minimum path with the energies projected onto the ε-axis. These figures should be compared with similar plots for isotopes of Z = 106 up to Z = 116 presented in ref. [4]).

4. Stabilities of Nuclei with $106 \leq Z \leq 128$ and $176 \leq N \leq 204$

The energy of the lowest minimum in the potential-energy surface gives the ground state mass. Based on the masses obtained, alpha decay half lives, and neutron and proton binding energies are estimated. Beta stabilities are also determined. The spontaneous-fission half-lives may also be found from the potential-energy surfaces provided one knows B, the inertial parameter associated with the barrier penetration. This parameter weighted by $A^{-5/3}$ has been evaluated in three alternative ways. The first evaluation corresponds to the microscopic calculation due to Sobiczewski et al.[12]), who found that the inertial parameters for the superheavy nuclei to cluster within 30% of a mean value. A second and semi-empirical estimate of $BA^{-5/3}$ is obtained from the calculated barriers and the experimental half-lives. These inertial parameters are also found to cluster within 30% of a mean value. A third estimate is due to Moretto and Swiatecki[13]). They used liquid-drop barriers modified by Myers-Swiatecki shell correction term[1]) and with the ground state masses and fission barriers adjusted to experimental values. Moretto and Swiatecki determined the mean value of $BA^{-5/3}$ for the actinides with only a 10% spread. It is found that all of these three estimates lie within 30% of each other, with the Moretto-Swiatecki estimate being the lowest. In our calculation of spontaneous-fission half-lives we have employed the latter estimate as giving the most conservative result. Based on the other estimates, some of the spontaneous-fission half-lives would be larger by one or two orders of magnitude.

The results are tabulated in tables 1 and 2 giving the stability for nuclei with $116 \leqslant Z \leqslant 128$ and $176 \leqslant N \leqslant 204$. For completeness we also show in table 3 the stability of nuclei around $Z = 114$ and $N = 184$ taken from ref. [4]). The values in the tables are summarized in the half-life contours of fig. 4. It is clear that any stability against spontaneous fission in this region is due to the extra binding resulting from the shell effect centered around $Z = 114$ and $N = 184 - 196$. On the other hand, the alpha half-lives are essentially determined by the liquid-drop model with modifications caused by the extra shell binding effect.† Thus the kinks in the curves occur when either the parent or the daughter nucleus is associated with a nucleon closed shell.

The uncertainties associated with the calculated half lives are discussed in detail in ref. [4]). The predicted energy barrier may be overestimated because of

---

†The interesting recent calculations by Muzychka (Joint Institute of Nuclear Research, Dubna, Preprint R7-4435, 1969) employing three alternative nuclear potentials namely the Woods-Saxon potentials of refs. [8]) and [10]) in addition to the potential employed by us, exhibit a discrepancy in the prediction of alpha half-lives which in the most unfavorable cases may be as large a factor as 10^8. On the whole, however, the discrepancy falls within the uncertainties expected according to ref. [4]). One may note that in the $^{294}110$ and $^{298}114$ cases the discrepancy is of the order of $10^4 - 10^5$. Finally one may note that the results based on our potential tend to fall between the predictions of the two alternative Woods-Saxon potentials employed.

the restricted parametrization, especially for large deformations. The estimation of B has an uncertainty of about 30%. The calculated ground-state masses for the known heavy nuclei are found[4]) to be good only to one or two MeV. All these errors enter into the half-life estimation exponentially, so that it is probable that our half-life values may be off by about four or five powers of ten. To this is then added the uncertainty due to the extrapolation of the nuclear potential to new mass regions. Nevertheless we expect the general pattern of the half-life contours to remain the same so long as Z = 114, N = 184 and N = 196 are associated with relatively large level spacings. Then the map should be useful as a guide in the search for superheavy nuclei.

5. Production of Superheavy Nuclei by Heavy-Ion Reactions

The production of superheavy nuclei by various methods is discussed in Ref. [4]) and [14]). At the moment it appears that the most promising method is associated with heavy-ion reactions.

With the presently available heavy-ion beams, the heaviest being that of ^{40}Ar, one finds that the compound nucleus produced is very neutron-deficient and therefore falls short of the island of stability. When heavier and hence more neutron-rich ions than ^{40}Ar can be accelerated, the prospect is improved for the production of superheavy nuclei. A plausible way of approach is to overshoot the $^{298}114$ doubly-closed shell nucleus and let various decay mechanisms lead up to a nucleus in its neighborhood. An extreme example is the reaction $^{238}U + ^{238}U$, as pointed out by Flerov[15]), Swiatecki[16]) and others. One may then expect that either a transfer reaction takes place, where the target captures a part of the projectile, or a compound nucleus is formed, which then undergoes fission. One hopes in this way to find products that are close enough to the center of the island of stability to have half-lives long enough for detection.

A possibility that is not so remote is furnished by reactions induced by the $^{86}_{36}Kr$ ion beam. In table 4 we show the compound nuclei that might be formed by bombarding various neutron-rich targets from Pb to Cm with ^{86}Kr. The question whether such a compound nucleus would be formed in the first place will be touched on below. At the moment let us assume that by emitting four neutrons a cold compound nucleus is obtained in the ground state. From fig. 4, it is apparent that for ^{208}Pb and ^{210}Po targets, the compound nucleus undergoes spontaneous fission instantaneously

and one may not expect to produce any superheavy nuclei. With targets heavier than ^{226}Ra, it turns out that the alpha half life is less than the spontaneous-fission half-life at each step (fig. 4). If the compound nucleus decays by emitting alpha particles all the way, in each case we end up with a long-lived superheavy nucleus. Any beta decay on the way, if competitive, will always help in reaching even longer-lived nuclei.

It is here appropriate again to emphasize that fig. 4 and the conclusions based thereon depend strongly on the magnitude of the N = 196 shell spacing which, as stated earlier, is a controversial result obtained on the basis of our specific potential model.

The above discussion of the production of superheavy nuclei is based on the assumption that the compound nucleus is formed in the reaction. This assumption may be subject to question for the following reasons. (1) There exist empirical indications that the cross-section of reactions, leading to the same compound nucleus, with a heavy projectile is reduced by several orders of magnitude compared with a reaction in which a lighter projectile is employed. (2) The large angular momentum introduced with the heavy projectile may cause the compound nucleus to fission directly rather than to decay into a stable minimum. This tendency is found in the liquid-drop model calculations, e.g., those of Cohen, et al.[17]). (3) Furthermore we know that any binding of a superheavy nucleus is due to the shell spacings connected with the doubly closed shells. The problem is somewhat open whether possibly this shell spacing is affected at the relatively large excitation of the compound nucleus in question.

Further studies of these problems are essential for any further attempts to make definite theoretical proposals for the production of superheavy nuclei.

Acknowledgments

We are much indebted to Dr. W. J. Swiatecki for stimulating and constructive discussions in all phases of this work. We are also grateful to Drs. G. T. Seaborg and S. G. Thompson for encouraging discussions. The co-operation of Drs. A. Sobiczewski, Z. Szymanski, S. Wycech, C. Gustafson, I. L. Lamm, P. Möller, and B. Nilsson is deeply appreciated.

The friendly hospitality of the Nuclear Chemistry Division and its excellent publication services are gratefully acknowledged.

References

1) W. D. Myers and W. J. Swiatecki, Nucl. Phys. 81 (1966) 1

2) H. Meldner and P. Röper, private communication to W. D. Myers and W. J. Swiatecki (see ref. [1])); H. Meldner, Arkiv Fysik 36 (1967) 593, Lawrence Radiation Laboratory Report UCRL-17801 (October 1968); A. Sobiczewski, F. A. Gareev, and B. N. Kalinkin, Phys. Letters 22 (1966) 500; V. M. Strutinsky and Yu. A. Muzychka, Proceedings International Conference of the Physics of Heavy Ions, 13-19 October (1966), Dubna, Vol. 2, p. 51; C. Y. Wong, Phys. Letters 21 (1966) 688; C. Gustafson, I. L. Lamm, B. Nilsson, and S. G. Nilsson, Arkiv Fysik 36 (1967) 613; P. A. Seeger and R. C. Perisho, A Model-based Mass Law and a Table of Binding Energies, Los Alamos Scientific Laboratory Report, LA-3751, UC-34, Physics, TID-4500 (1967)

3) S. G. Nilsson, J. R. Nix, A. Sobiczewski, Z. Szymanski, S. Wycech, C. Gustafson and P. Möller, Nucl. Phys. A115 (1968) 545

4) S. G. Nilsson, C. F. Tsang, A. Sobiczewski, Z. Szymanski, S. Wycech, C. Gustafson, I. L. Lamm, P. Möller, and B. Nilsson, Nucl. Phys. A131 (1969) 1; S. G. Nilsson, Lawrence Radiation Laboratory Report UCRL-18355-Rev. (Berkeley, Sept. 1968); S. G. Nilsson, S. G. Thompson, and C. F. Tsang, Phys. Letters 28B (1969) 548

5) V. M. Strutinsky, Nucl. Phys. A95 (1967) 420; V. M. Strutinsky, Nucl. Phys. A122 (1968) 1

6) C. F. Tsang, Ph.D. Thesis, University of California Lawrence Radiation Laboratory Report UCRL-18899

7) W. D. Myers and W. J. Swiatecki, Lysekil Symposium, Sweden, 1966, (Almqvist and Wiksell, Stockholm, 1967), p. 393, and Arkiv Fysik, 36 (1967) 593

8) E. Rost, Phys. Letters 26B (1967) 184

9) M. Bolsterli, E. O. Fiset, and J. R. Nix, Los Alamos Scientific Laboratory Report LA-DC-10249 (1969)

10) V. A. Chepurnov, Yadernaya Fizika, 6 (1967) 955

11) Yu. A. Muzychka, Phys. Letters 28B (1969) 539

12) A. Sobiczewski, Z. Szymanski, S. Wycech, S. G. Nilsson, J. R. Nix, C. F. Tsang, C. Gustafson, I. L. Lamm, P. Möller, and B. Nilsson, Nucl. Phys. A131 (1969) 67

13) L. G. Moretto and W. J. Swiatecki, private communication

14) G. T. Seaborg, Ann. Rev. Nucl. Sci. 18 (1968) 53-152

15) G. N. Flerov, Joint Institute for Nuclear Research, Dubna, preprint E7-4207 (1968)

16) W. J. Swiatecki, Research Progress Meeting Talk, Lawrence Radiation Laboratory, Berkeley, February 1968

17) S. Cohen, F. Plasil, and W. J. Swiatecki, Proc. Third Int. Conf. on Reactions between Complex Nuclei, University of California Press, Berkeley (1963) 325

Figure Captions

Fig. 1. Single-proton level diagram for spherical potential. Parameters are fitted[4]) to reproduce observed deformed single-particle level order at $A \approx 165$ and 242, and are extrapolated linearly to the other regions. E Rost's predicted level order[8]) for A = 298 is exhibited for comparison.

Fig. 2. Analogous to fig. 1, valid for neutrons.

Fig. 3a. Total energy minimized with respect to ε_4 for each ε as function of ε for isotopes of Z = 116 with N around 184.

Fig. 3b. Same as fig. 3a for isotopes of Z = 116 with N around 196.

Fig. 3c. Same as fig. 3a for isotopes of Z = 118 with N around 184.

Fig. 3d. Same as fig. 3a for isotopes of Z = 118 with N around 196.

Fig. 3e. Same as fig. 3a for isotopes of Z = 120 with N around 184.

Fig. 3f. Same as fig. 3a for isotopes of Z = 120 with N around 196.

Fig. 3g. Same as fig. 3a for isotopes of Z = 122 with N around 184.

Fig. 3h. Same as fig. 3a for isotopes of Z = 122 with N around 196.

Fig. 3i. Same as fig. 3a for isotopes of Z = 124 with N around 184.

Fig. 3j. Same as fig. 3a for isotopes of Z = 124 with N around 196.

Fig. 3k. Same as fig. 3a for isotopes of Z = 126 with N around 184.

Fig. 3ℓ. Same as fig. 3a for isotopes of Z = 126 with N around 196.

Fig. 3m. Same as fig. 3a for isotopes of Z = 128 with N around 184.

Fig. 3n. Same as fig. 3a for isotopes of Z = 128 with N around 196.

Fig. 4. Contours of theoretical half-lives for $106 \leqslant Z \leqslant 128$ and $176 \leqslant N \leqslant 204$. The thick dark lines are contours of spontaneous-fission half-lives. The broken lines are contours of alpha half-lives. Beta stable nuclei are shaded.

List of Tables

nucleus that can be reached is shown in the fourth column with its major mode of decay. Under the further assumption that the nucleus in column 4 undergoes beta decay the superheavy nucleus shown in the fifth column is obtained with its major mode of decay as indicated.

Table 1

Z \ N	176	177	178	179	180	181	182	183	184	185	186	187	188	189	190
128									277.71 10^{-2}_{α} (6.4) 10^{-7}_{β} (14.74) -0.74	278.42	278.93 10^{-3}_{α} (6.2) 10^{-9}_{α} (15.64) 7.90, -0.42	279.67	279.90 10^{-4}_{α} (6.0) 10^{-8}_{β} (15.62) 7.84, -0.09	281.23	281.64 10^{-5}_{α} (5.7) 10^{-8}_{β} (15.56) 7.69, 0.03
127									269.68	270.56	270.98	272.13	272.52	274.02	274.55
126							260.54 10^{-6}_{α} (5.5) 10^{-7}_{β} (14.70) -0.39	260.69	260.12 0.1α (7.2) 10^{-6}_{α} (13.94) 8.44, -0.08	261.35	261.85 10^{-2}_{α} (7.2) 10^{-8}_{α} (15.05) 7.57, 0.24	263.26	263.52 10^{-3}_{α} (7.0) 10^{-7}_{α} (14.83) 7.51, 0.56	265.47	266.18 10^{-2}_{α} (6.9) 10^{-7}_{α} (14.57) 7.36, 0.47
125							252.86	253.17	252.95	254.15	254.80	256.38	257.09	258.92	259.75
124					243.41 (10^{-6}_{α}) (5.2) 10^{-6}_{α} (13.78) +0.22	244.07	243.95 10^{-3}_{α} (6.2) 10^{-5}_{α} (13.32) 8.19, +0.32	244.43	244.37 10^{2}_{α} (7.9) 10^{-5}_{α} (13.00) 8.13, 0.64	245.73	246.56 10α (8.0) 10^{-7}_{α} (14.12) 7.24, 0.98	248.10	249.15 1α (7.9) 10^{-6}_{α} (13.88) 7.19, 1.29	251.16	252.18 0.1α (7.9) 10^{-6}_{α} (13.62) 7.05, 1.61
123					236.34	236.92	236.98	237.61	237.72	239.26	240.25	242.14	243.18	245.33	246.50
122			227.20 $\Pi 0^{-1}_{\alpha}$ (5.0) 10^{-6}_{β} (13.08) +0.53	228.14	228.20 10^{-5}_{β} (5.5) 10^{-5}_{α} (13.09) 8.01, +0.71	228.96	228.94 10^{-2}_{β} (7.0) 10^{-4}_{α} (12.47) 8.09, +1.02	229.74	230.01 10^{0}_{β} (8.0) 10^{-3}_{α} (12.15) 7.80, 1.13	231.70	232.87 10^{1}_{β} (8.0) 10^{-6}_{α} (13.29) 6.90, 1.66	234.93	236.14 10^{2}_{β} (8.9) 10^{-5}_{α} (13.04) 6.86, 1.99	238.43	239.78 10α (8.2) 10^{-5}_{α} (12.76) 6.72, 2.31
121			220.44	221.40	221.62	222.54	222.67	223.62	224.05	225.92	227.24	229.47	230.84	233.30	234.80
120	211.69 (10^{-5}_{α}) (3.9)	212.68	212.68 (10^{-5}_{α}) (5.0) 8.07, +1.17	213.77	214.04 10^{-3}_{β} (6.3) 10^{-4}_{α} (12.04) 7.80, +1.45	215.13	215.43 1α (7.3) 10^{-3}_{α} (11.53) 7.77, +1.76	216.55	217.15 1γ (9.0) 10^{-2}_{α} (11.22) 7.47, +2.08	219.17	220.47 10γ (9.0) 10^{-4}_{α} (12.57) 6.47, 2.41	223.06	224.40 10^{2}_{β} (6.9) 10^{-6}_{α} (12.10) 6.53, 2.73	227.23	228.90 10^{-1}_{β} (8.8) 10^{-2}_{α} (11.83) 6.40, 3.05
119		206.42	206.56	207.77	208.20	209.44	209.90	211.19	211.94	214.14	215.79	218.35	220.04	222.84	224.66
118			199.57 (10^{-5}_{α}) (5.0) +1.93	200.96	201.47 10^{-2}_{β} (6.9) 10^{-2}_{α} (10.92) 7.56, +2.18	202.89	203.50 10^{2}_{β} (7.6) 0.1α (10.54) 7.46, +2.49	204.95	205.87 10^{0}_{β} (9.2) 1α (10.26) 7.15, +2.82	208.23	210.06 10^{0}_{β} (9.2) 10^{-3}_{α} (11.43) 6.24, 3.15	212.78	214.64 10^{2}_{β} (9.2) 10^{-2}_{α} (11.15) 6.21, 3.47	217.59	219.59 10^{2}_{β} (9.3) 10^{-2}_{α} (10.8-) 6.07
117			194.21	195.68	196.36	197.92	198.70	200.32	201.40	203.93	205.92	209.80	210.82		
116			188.13 10^{-1}_{α} (5.0)	189.76	190.53 10^{6}_{α} (6.5) 7.30,	192.26	193.18 10^{6}_{γ} (7.9 7.15,	194.95	196.20 10^{12}_{γ} (9.3) 6.82	198.89	201.06 10^{12}_{γ} (9.3) 5.90	204.11	206.29 10^{12}_{γ} (9.3) 5.89		

TBL-693-340

Table 2

Z \ N	190	191	192	193	194	195	196	197	198	199	200	201	202	203	204
128					285.13 0.1α (6.8) 10^{-2}_{β} (14.65) ,0.85	286.73	287.81 10^{-2}_{β} (5.5) 10^{-6}_{β} (14.40) 6.99, 1.16	290.37	292.32 10^{-5}_{β} (3.4) 10^{-8}_{β} (15.60) 6.12, 1.47	295.29	297.21 10^{-11}_{β} (2.0) 10^{-9}_{β} (15.34) 6.15, 1.78	300.21	302.05 10^{-12}_{β} 10^{-7}_{β} (14.62) 6.23, 2.17		
127					278.60	280.44	281.68	284.41	286.50	289.64	291.70	294.97	296.93	300.08	
126	265.47 1α (7.9) 10^{-7}_{β} (14.44) ,0.68	267.22	268.05 1α (7.2) 10^{-6}_{β} (14.12) 7.24, 1.20	269.92	270.98 1α (6.8) 10^{-6}_{β} (13.83) 7.01, 1.51	272.89	274.28 10α (6.5) 10^{-5}_{β} (13.56) 6.68, 1.82	277.17	279.44 10^{-4}_{β} (4.7) 10^{-8}_{β} (14.79) 5.80, 2.12	282.73	284.95 10^{-8}_{β} (3.0) 10^{-7}_{β} (14.53) 5.85, 2.44	288.39	290.66 $\leq 10^{-13}_{\beta}$ (1.6 10^{-6}_{β} (14.07) 5.8, 2.76	293.96	296.13 10^{-5}_{β} (13.14
125	263.06	260.96	264.96	263.98	265.20	267.27	268.81	271.86	274.27	277.73	280.10	283.79	286.13	289.72	292.03
124	251.50 10α (8.3) 7.09, 1.61	253.57	254.72 10^{2}_{β} (8.0 10^{-5}_{β} (13.15) 6.92, 1.93	256.91	258.29 10^{4}_{β} (7.8) 10^{-5}_{β} (12.86) 6.69, 2.23	260.51	262.22 10^{5}_{β} (7.4) 10^{-4}_{β} (12.59) 6.36, 2.55	265.43	268.01 10^{-3}_{β} (5.7) 10^{-6}_{β} (13.82) 5.49, 2.86	271.62	274.16 10^{-6}_{β} (3.9) 10^{-6}_{β} (13.54) 5.53, 3.18	278.01	280.54 10^{-11}_{β} (2.5) 10^{-5}_{β} (13.14) 5.54, 3.48	284.35	287.02 10^{-17} 10^{-4}_{β} (12.43) 5.57, 3.64
123	248.82	248.05	249.36	251.71	253.23	255.62	257.48	260.85	263.58	267.35	270.05	274.05	276.73	280.70	283.48
122	239.14 10^{6}_{α} (9.0) ,2.33	241.53	243.00 10^{6}_{α} (8.9) 10^{-4}_{β} (12.24) 6.6, 2.64	245.51	247.20 10^{5}_{α} (8.6) 10^{-3}_{β} (11.95) 6.38, 2.96	249.75	251.76 1y (8.2) 10^{-2}_{β} (11.68) 6.06, 3.28	255.29	258.19 10^{3}_{α} (6.4) 10^{-5}_{β} (12.92) 5.17, 3.58	262.11	264.97 10^{-6}_{β} (4.7) 10^{-5}_{β} (12.63) 5.21, 3.91	269.14	271.99 10^{-7}_{β} (3.1) 10^{-4}_{β} (12.42) 5.22, 4.20	276.18	279.05 10^{-15}_{β} (2.1) 10^{-3}_{β} (11.98) 5.20, 4.58
121	234.18	236.72	238.35	241.02	242.87	245.56	247.75	251.42	254.48	258.57	261.59	265.91	268.90	273.34	276.34
120	228.91 10^{9}_{γ} (9.4) ,4.09	231.02	232.82 10^{4}_{α} (9.2) 10^{-3}_{β} (11.51) 6.27, 3.91	235.05	237.05 10^{4}_{γ} (9.2) 10^{-2}_{β} (11,00) 6.07, 4.72	240.51	242.84 10^{6}_{γ} (8.7) 0.1α (10.71) 5.74, 4.04	246.68	249.91 10^{3}_{α} (7.0) 10^{-4}_{β} (11.98) 4.84, 4.35	254.15	257.34 1α (5.2) 10^{-1}_{β} (11.68) 4.88, 4.66	264.81	264.98 10^{-2}_{β} (11.26 4.90, 4.98	269.57	272.71 10^{-11}_{β} (12.4 (10.34 4.98
119	224.01	226.07	228.04	231.02	234.08	237.10	239.49	243.50	246.97	251.38	254.71	259.46	262.67		
118	219.05 10^{9}_{α} (9.3)	222.11	224.22 10^{10}_{γ} (9.9) 5.96, 4.16	227.37	229.70 10^{10}_{γ} (9.3) 10α (10.00) 5.74, 4.46	232.87	235.52 10^{12}_{γ} (9.0) 10α (9.73) 5.42, 4.79	239.69	243.23 10^{6}_{γ} (7.5) 10^{-2}_{β} (10.99) 4.53, 5.10	247.80	251.29 10α (5.7) 10^{-1}_{β} (10.69) 4.58	256.08	259.57 10^{-6}_{β} (4.0) 4.58		
117		218.83	221.09	224.40	226.87	230.21	233.02	237.35	241.04						
116			217.26 10^{15}_{γ} (9.4)	220.71	223.36 10^{16}_{γ} (9.5) 5.42,	226.84	229.81 10^{18}_{γ} (9.2) 5.10,	234.30	238.17 10^{10}_{γ} (7.5) 4.20,						

NBL-6053-330

Table 3

Z \ N	178	179	180	181	182	183	184	185	186	187	188	189
112	187.87 (1ms) (5.8) 1s (10.14)		190.56 1d (7.1) 1min (9.92)		193.14 10^3y (8.3) 10s (9.71)		196.42 10^{11}y (9.4) 1min (9.58)		201.30 10^{11}y (9.4) 0.1s (10.53)		20[illegible] 1s (10.24)	
111	186.07		189.79 10min (8.89)		188.81 10h (8.58)		192.45 1d (8.41)		197.66 10s (9.39)		203.2 10min (9.11)	
110	178.01 1min (9.4)	180.09	181.00 10^2y (7.0) 10d (7.97)	183.17 1y (7.71)	184.41 10^9y (8.3) 1y (7.55)	186.56 10^2y (7.20)	188.34 10^{16}y (9.6) 10y (7.40)	191.29 100d (7.87)	193.88 10^{15}y (9.4) 1d (8.34)	197.32 9h (8.49)	199.84 10^{14}y (9.4) 10d (8.09)	203. 2 10d (8.00)
109	174.44		177.84 10y (7.33)		181.57 10^3y (6.80)		185.84 10^5y (6.58)		191.71 1y (7.53)		198.00 10y (7.29)	
108	170.60 1s (8.1)	173.03	174.43 10d (5.7) 1y (7.46)	176.93 10^2y (7.17)	178.51 10^6y (6.9) 10^3y (6.83)	180.99 10^4y (6.52)	183.11 10^{13}y (8.1) 10^4y (6.54)	186.40 10^2y (7.10)	189.32 10^{13}y (8.1) 1y (7.50)	193.09 100d (7.64)	19[illegible].94 10^{12}y (8.1) 10y (7.24)	199.3 10y (7.1[illegible])
107	168.08		172.34 10y (7.04)		176.83 10^5y (6.38)	179.47 10^9y (6.63)	181.75 10^7y (6.03)		188.28 10^2y (6.98)		19[illegible].23 10^3y (6.72)	
106	164.04 (1ms) (7.2) 10y (7.20)	167.33	169.23 10min (4.3) 10^2y (6.84)	172.04 10^4y (6.40)	174.14 10^4y (6.5) 10^6y (6.14)	176.87 10^9y (6.63)	179.39 10^{10}y (6.8) 10^8y (6.76)	183.01 10^5y (6.24)	186.27 10^{10}y (6.7) 10^2y (6.73)	190.36 10^2y (6.86)	193.[illegible] 10^9y (6.8) 10^4y (6.[illegible])	197.99 10^4y (7.[illegible])
105	160.86		168.02	171.10	173.29	176.18	178.87 10^{11}y (5.24)	182.66	186.08 10^3y (6.21)		193.[illegible]	
104	1[illegible].97 10^4y (6.38)	165.21	167.37 10s (7.2) 10^4y (6.23)	168.81	171.20 10^2y (6.3) 10^8y (6.[illegible])	174.34	177.11 10^8y (5.8) 10^{13}y (4.89)	181.07 10^9y (5.39)	184.66 10^9y (5.9) 10^6y (6.[illegible])	189.10	192.[illegible] 10^7y (6.[illegible])	
103					171.20	174.49	177.44					
102					169.79 10d (3.9) 10^{11}y (4.97)	173.2[illegible]	176.37 10^7y (5.3)					

XBL 699-1481

Table 4.

Production of Superheavy Nuclei by $^{86}_{36}Kr_{50}$ Projectile

Target				Compound Nucleus		After emitting 4n		Longest-lived nuclei reached after competition between s.f. and successive α-decay			After β-decay		
	A	Z	N	Z	N	Z	N	Z	N	Major Decay	Z	N	Major Decay
Pb	208	82	126	118	176	118	172		(s.f)				
Po	210	84	126	120	176	120	172		(s.f)				
Rn													
Ra	226	88	138	124	188	124	184	118	178	$\alpha(10^{-3}s)$	112	184	$\alpha(10^{4}y)$
Th	232	90	142	126	192	126	188	116	178	$\alpha(10^{-1}s)$	112	182	$\alpha(10^{2}y)$
U	238	92	146	128	196	128	192	114	178	$\alpha(10^{3}s)$	110	182	$\alpha(10^{2}y)$
Pu	244	94	150	130	200	130	196	114	180	$\alpha(10^{4}s)$	112	182	$\alpha(10^{2}y)$
Cm	248	96	152	132	202	132	198	114	180	$\alpha(10^{4}s)$	112	182	$\alpha(10^{2}y)$

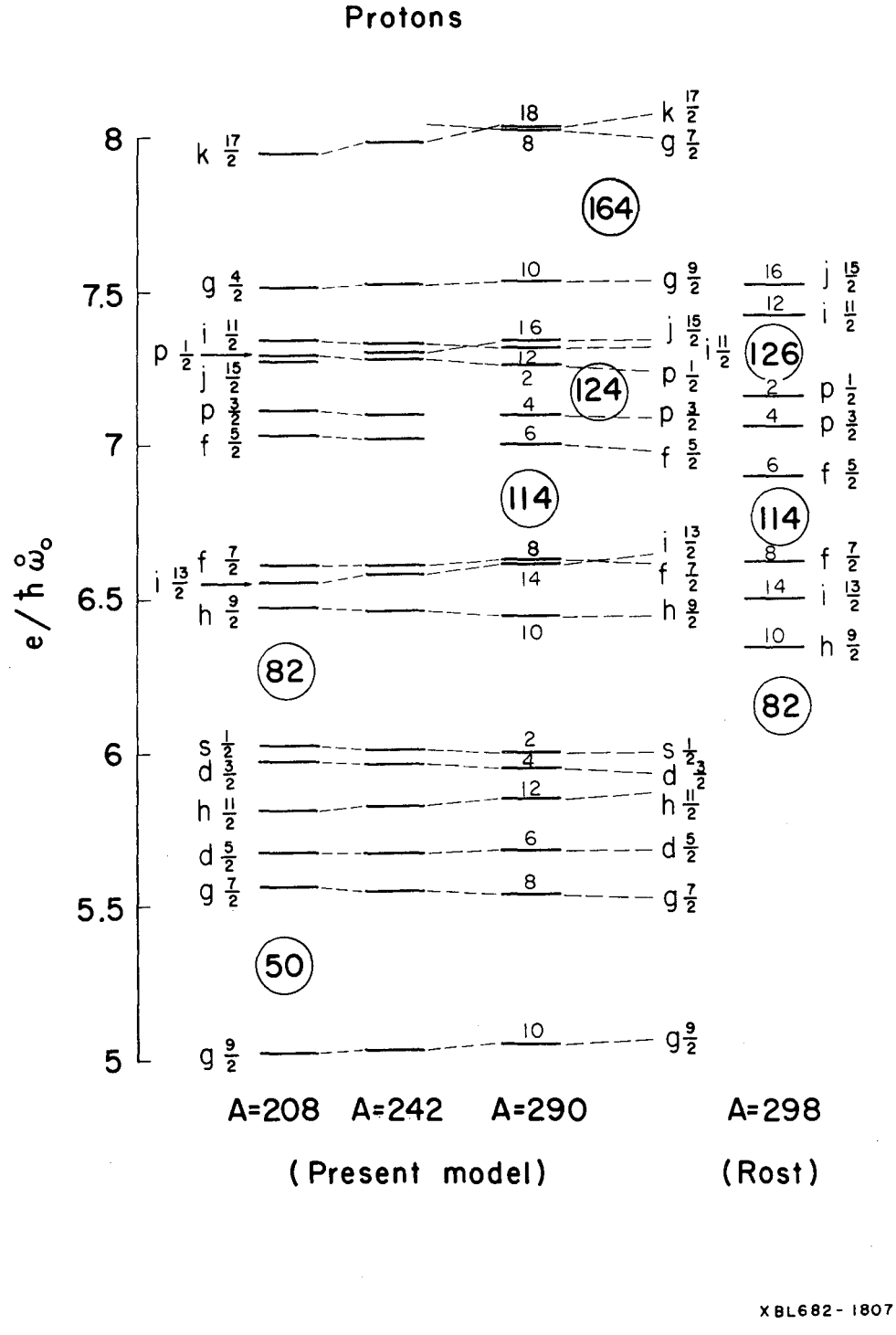
Protons
e / ħω₀
8
7.5
7
6.5
6
5.5
5
k 17/2
g 4/2
i 11/2
p 1/2
j 15/2
p 3/2
f 5/2
f 7/2
i 13/2
h 9/2
s 1/2
d 3/2
h 11/2
d 5/2
g 7/2
g 9/2
18
8
10
16
12
2
4
6
14
164
124
114
82
50
126
A=208
A=242
A=290
A=298
(Present model)
(Rost)
XBL682-1807

Fig. 1.

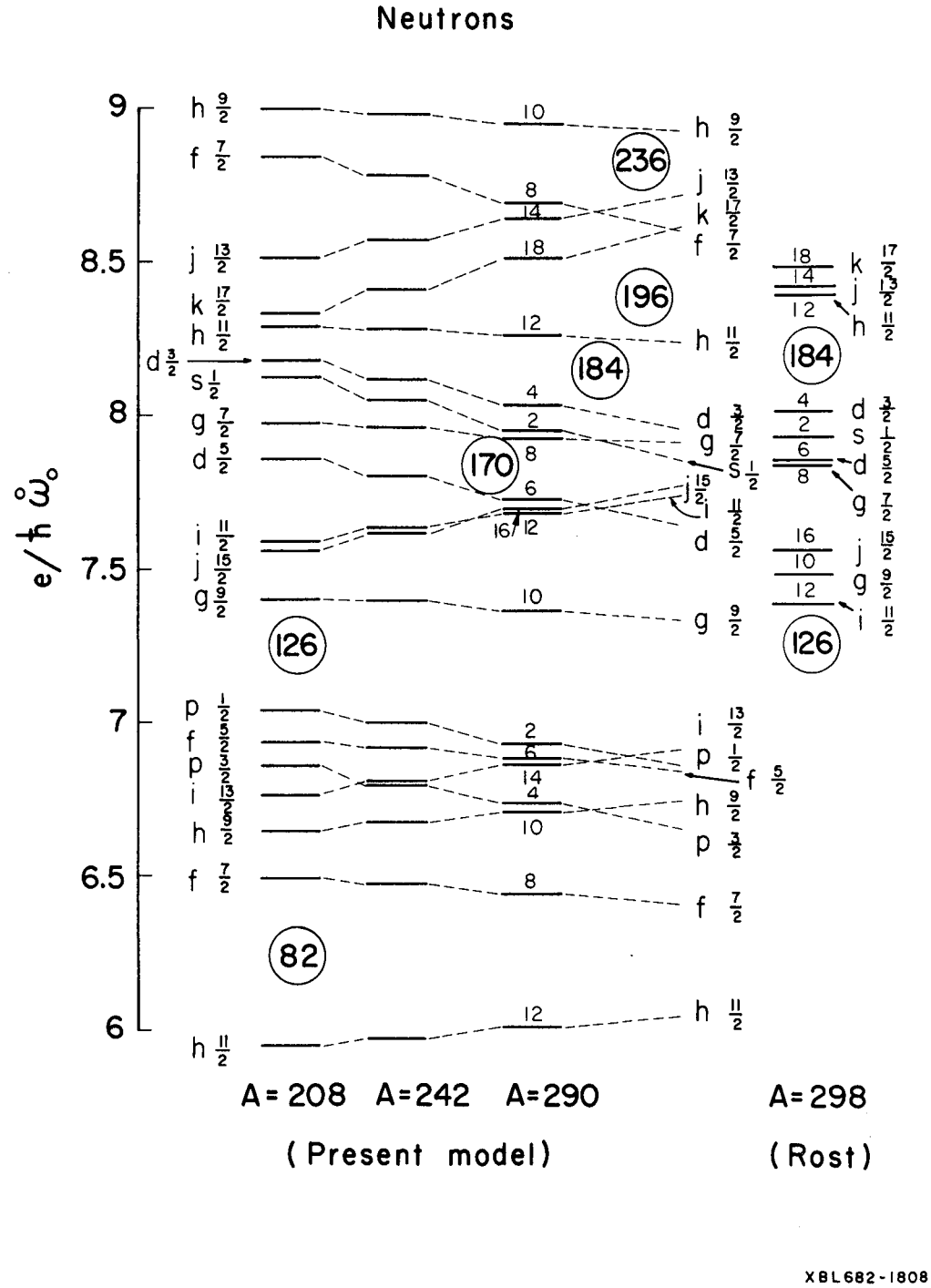
Neutrons
e/ħω₀
9
8.5
8
7.5
7
6.5
6
236
196
184
170
126
82
A= 208
A=242
A=290
A=298
(Present model)
(Rost)
XBL682-1808

Fig. 2.

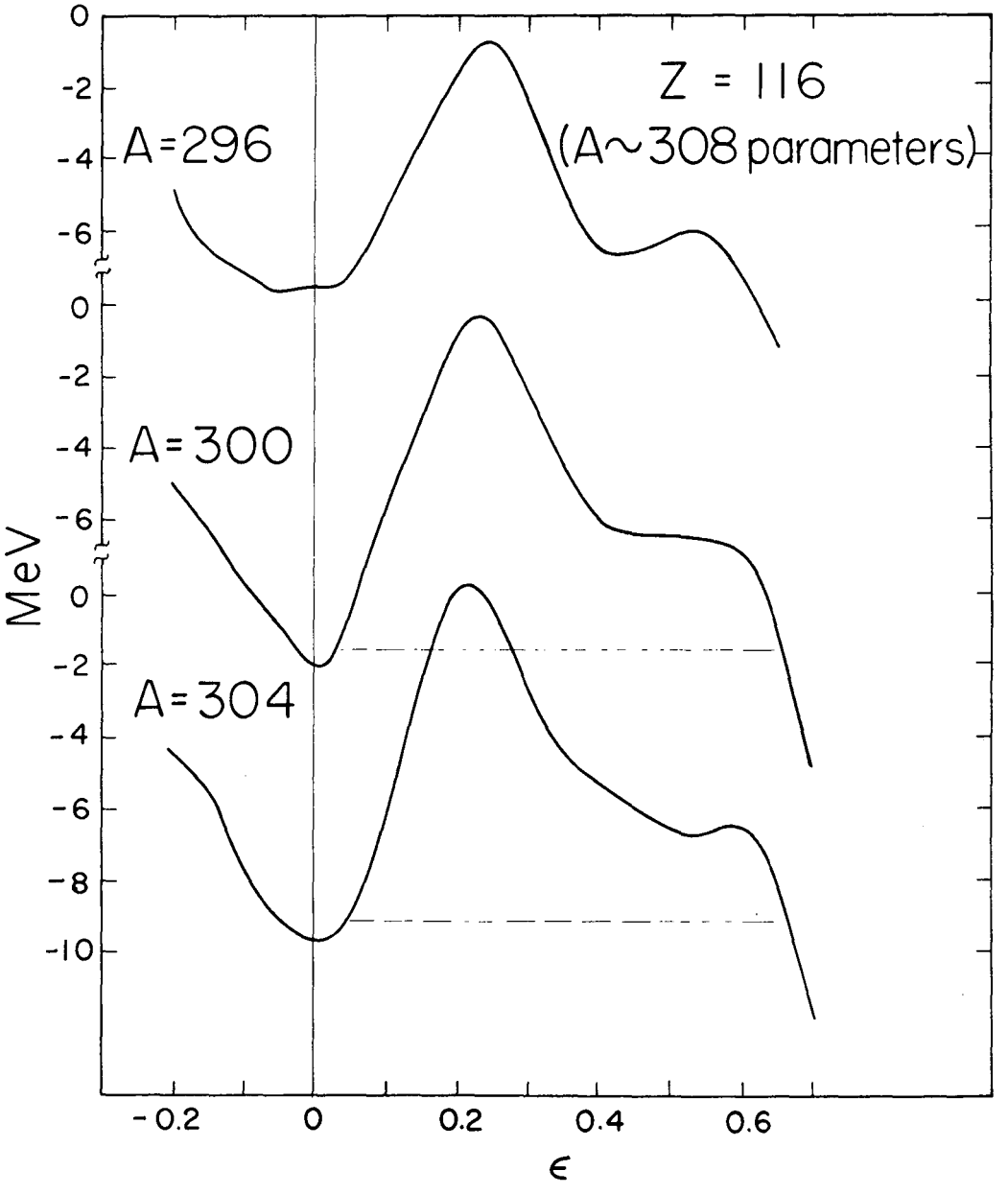

XBL692-2077

Fig. 3a.

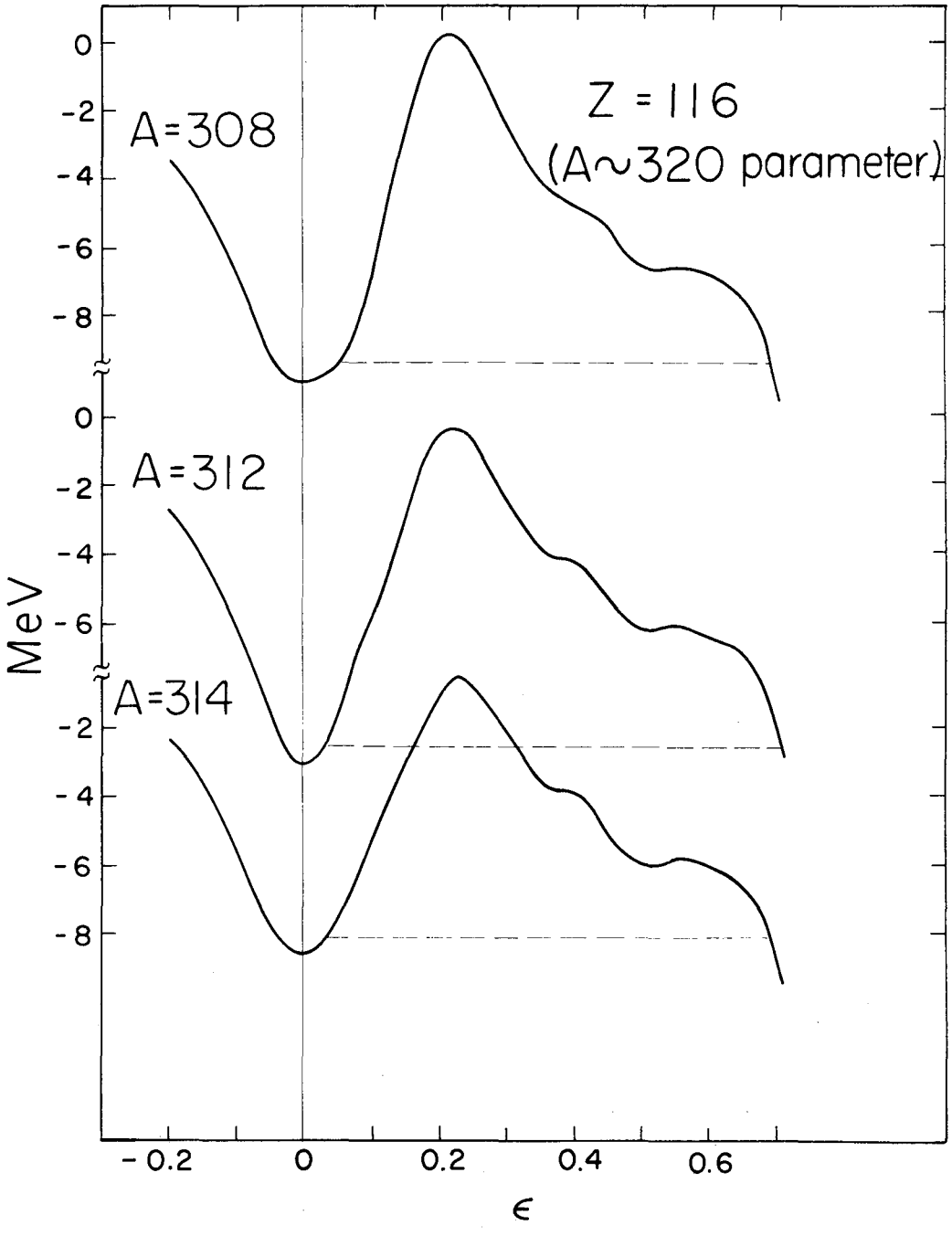
Z = 116
(A~320 parameter)
A=308
A=312
A=314
MeV
0
-2
-4
-6
-8
-0.2
0
0.2
0.4
0.6
ϵ
XBL692-2084

Fig. 3b.

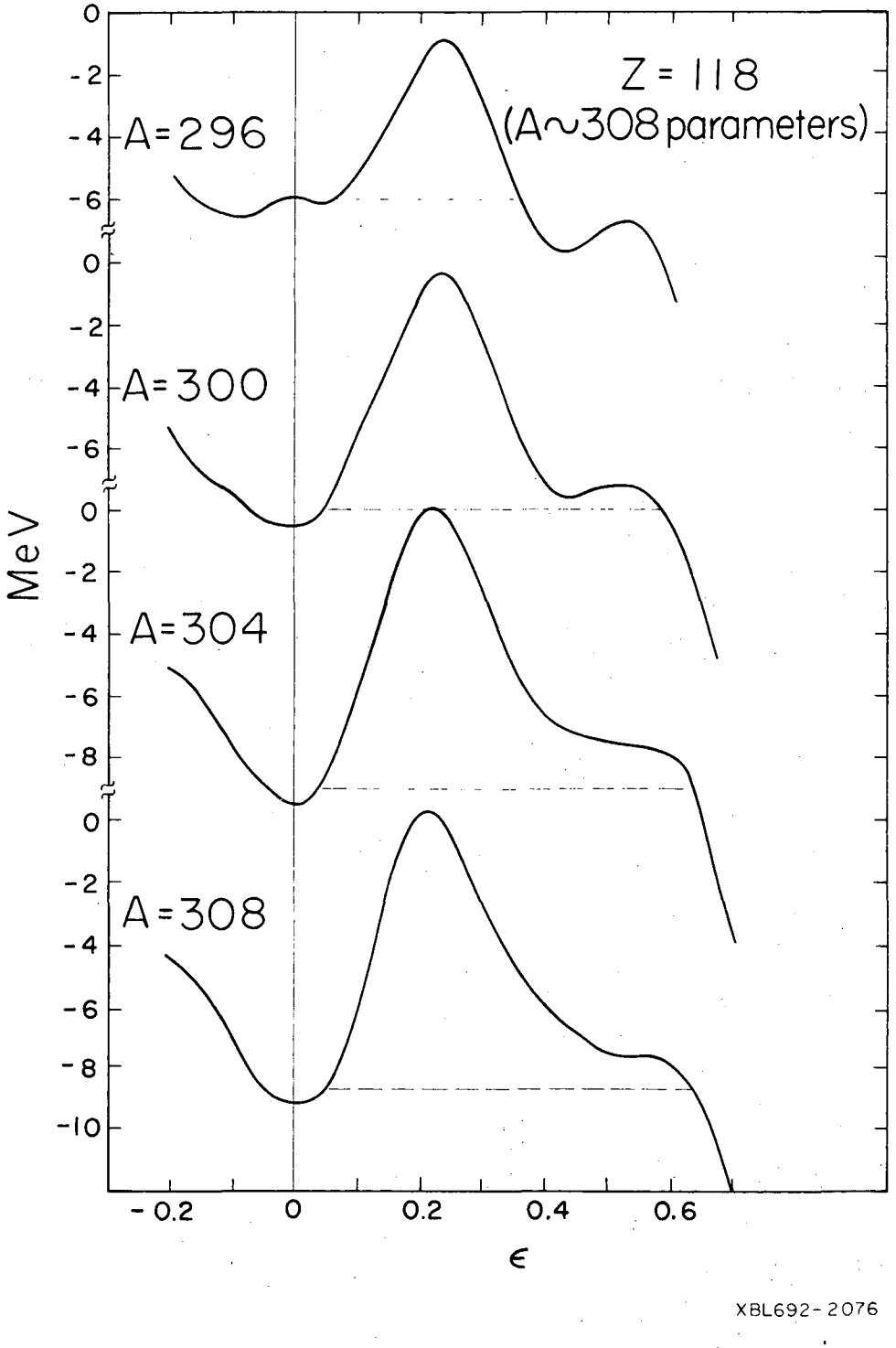
Z = 118
(A~308 parameters)
A=296
A=300
A=304
A=308
MeV
0
-2
-4
-6
-8
-10
-0.2
0
0.2
0.4
0.6
ϵ
XBL692-2076

Fig. 3c.

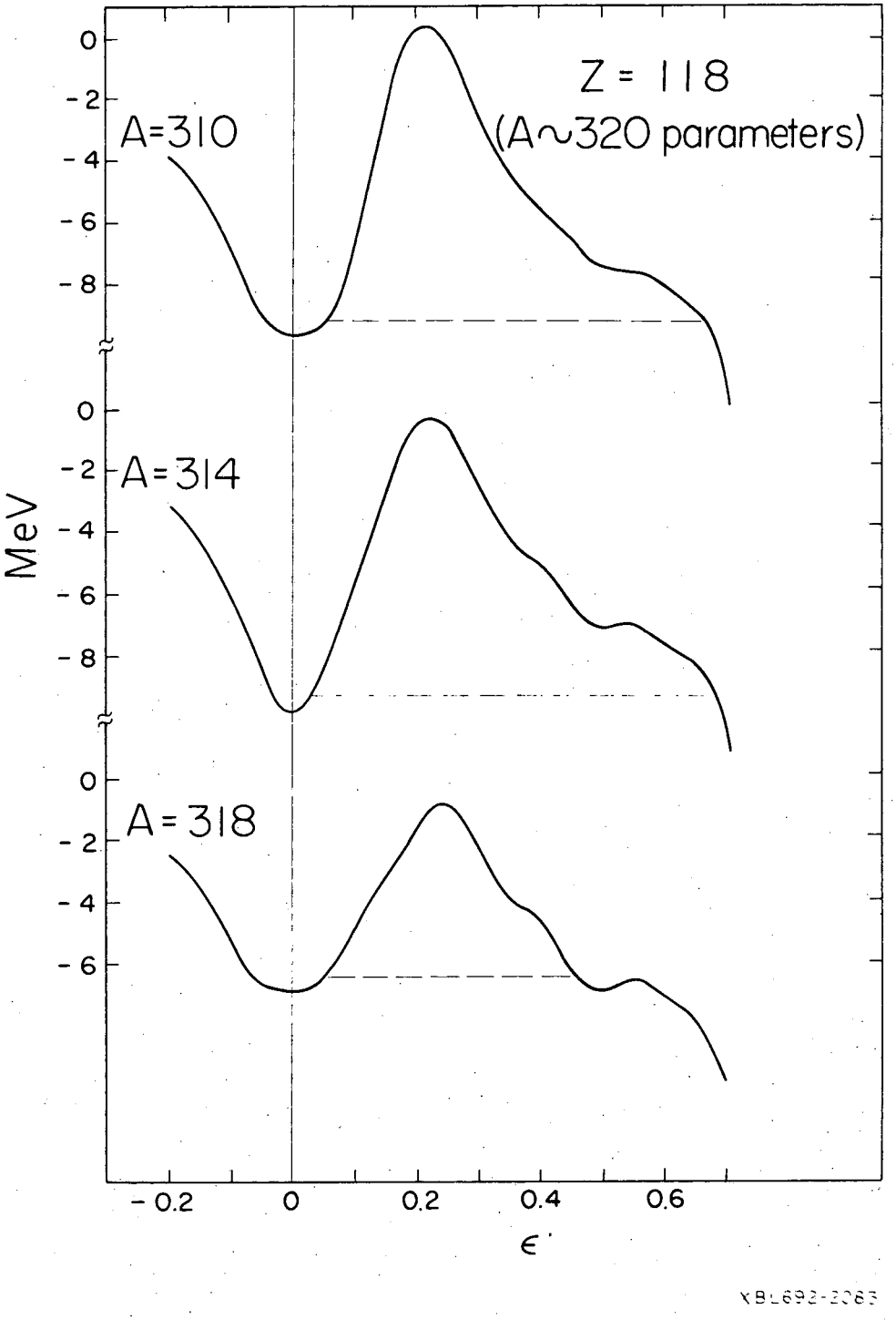

Fig. 3d.

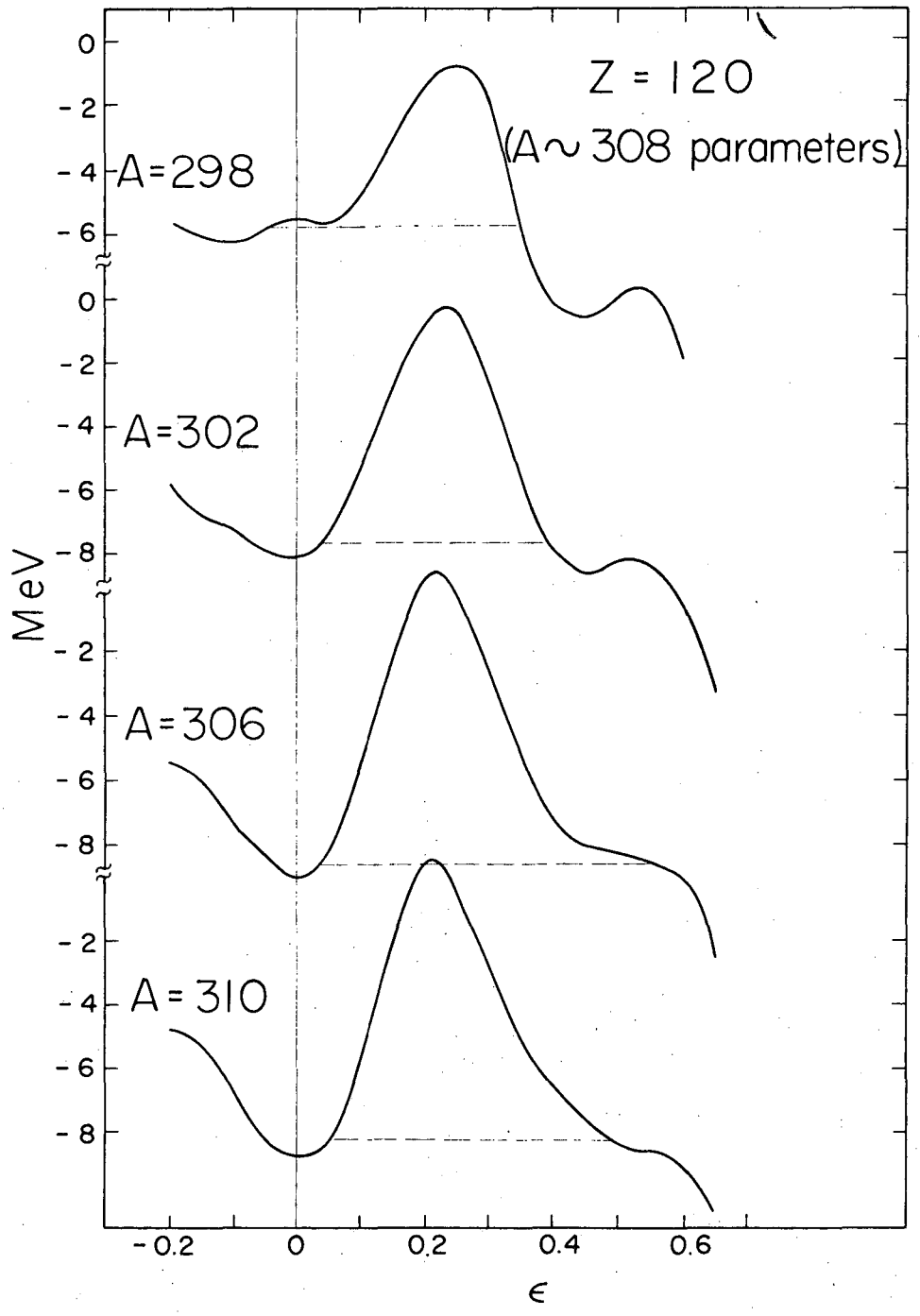
Z = 120
(A~ 308 parameters)
A=298
A=302
A=306
A = 310
MeV
0
-2
-4
-6
-8
-0.2
0
0.2
0.4
0.6
ϵ
XBL692-2075

Fig. 3e.

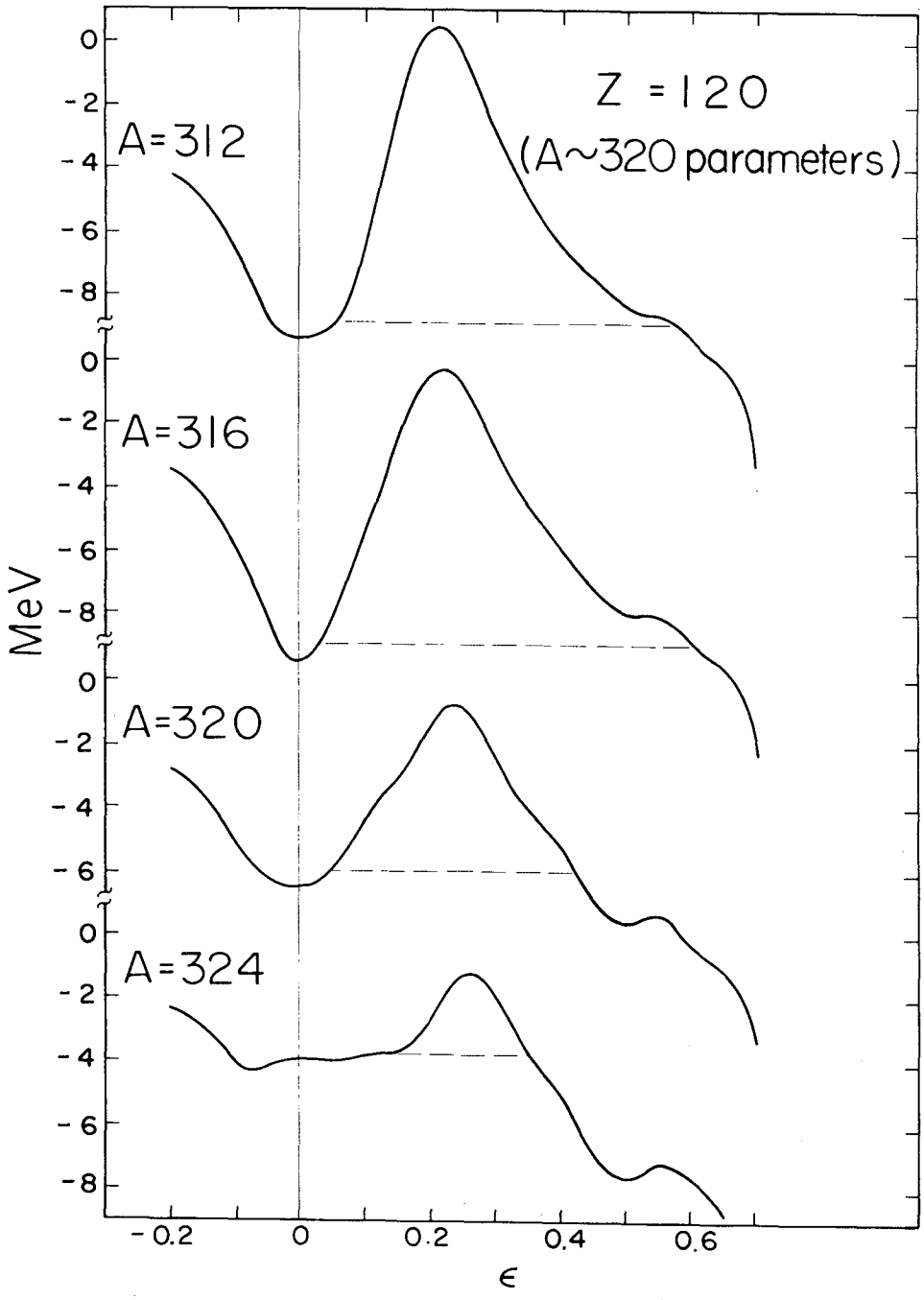
Z = 120
(A~320 parameters)
A=312
A=316
A=320
A=324
MeV
0
-2
-4
-6
-8
-0.2
0
0.2
0.4
0.6
ϵ
XBL692-2082

Fig. 3f.

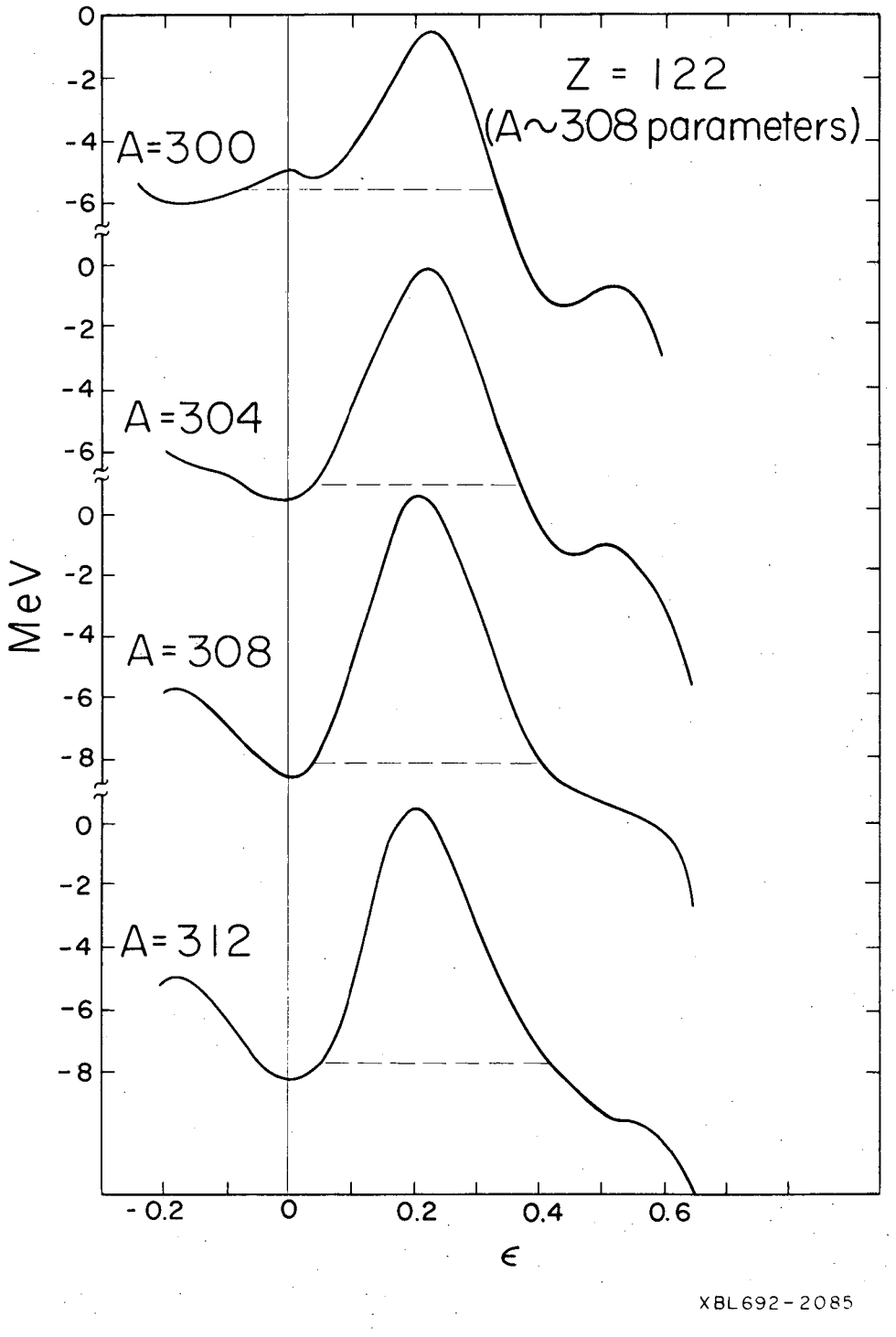
Z = 122
(A~308 parameters)
A=300
A=304
A=308
A=312
MeV
0
-2
-4
-6
-8
-0.2
0
0.2
0.4
0.6
ϵ
XBL692-2085

Fig. 3g.

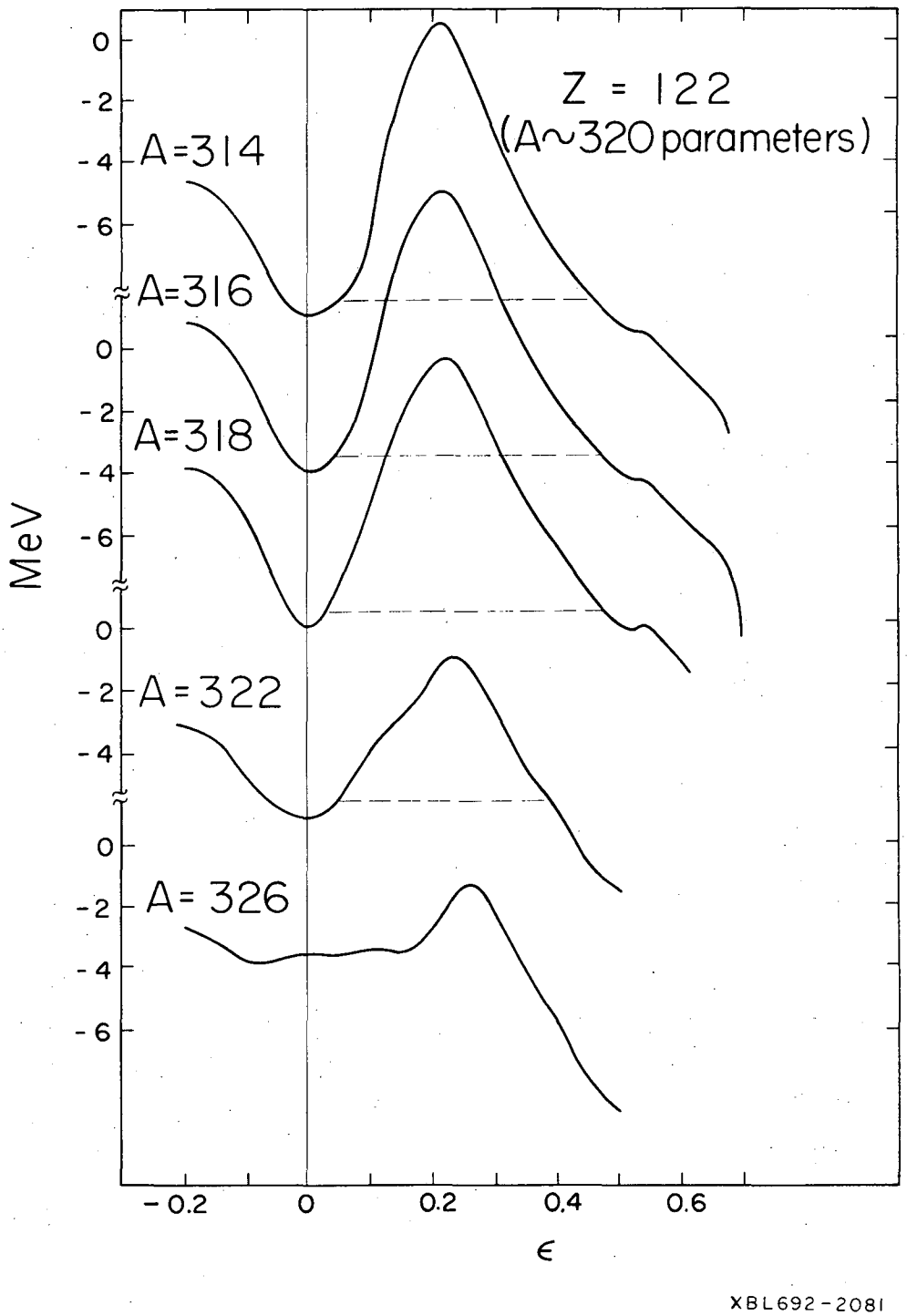
Z = 122
(A~320 parameters)
A=314
A=316
A=318
A=322
A= 326
MeV
0
-2
-4
-6
-0.2
0
0.2
0.4
0.6
ϵ
XBL692-2081

Fig. 3h.

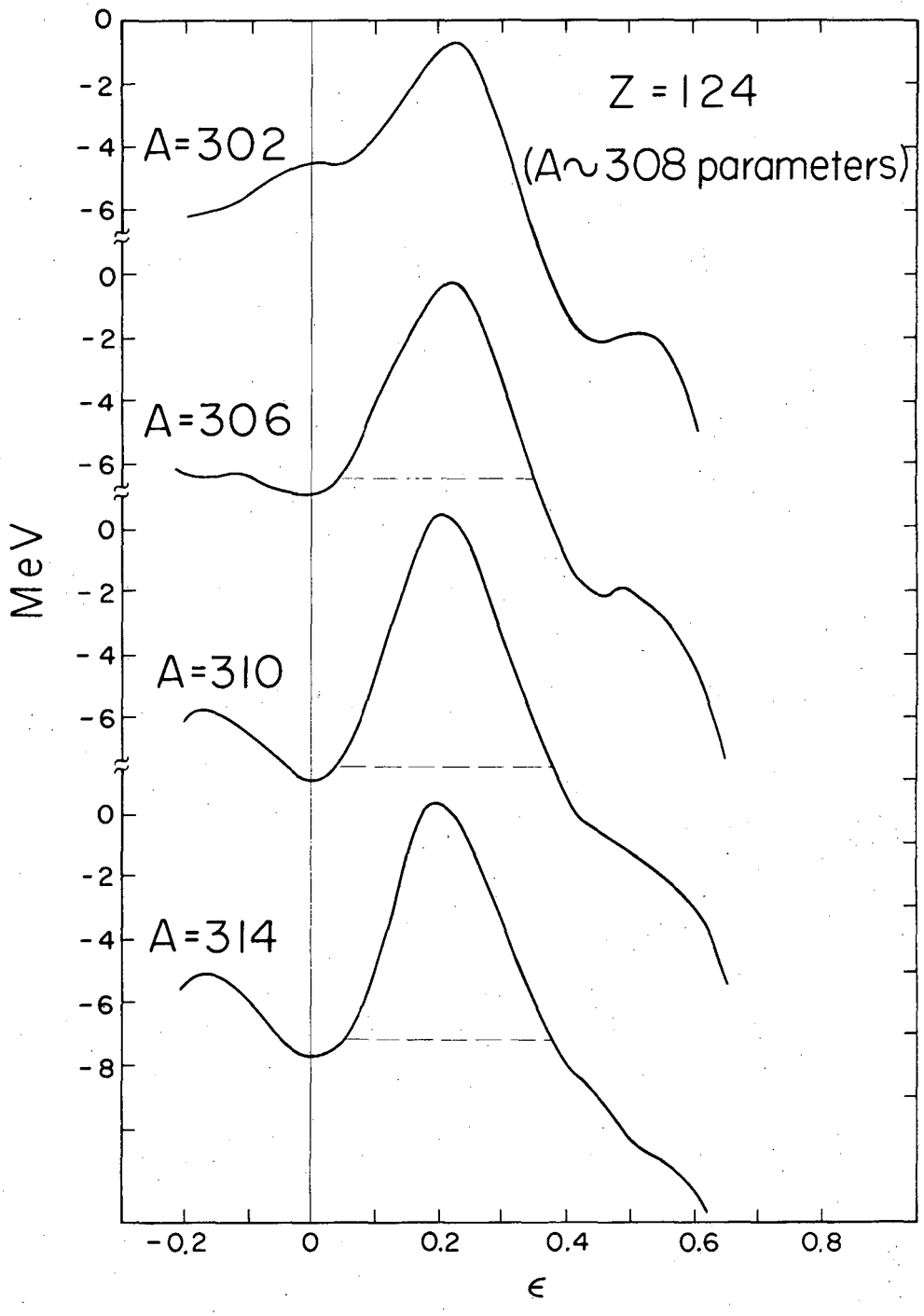
Z = 124
(A~308 parameters)
A=302
A=306
A=310
A=314
MeV
0
-2
-4
-6
-8
-0.2
0
0.2
0.4
0.6
0.8
ϵ
XBL692-2086

Fig. 3i

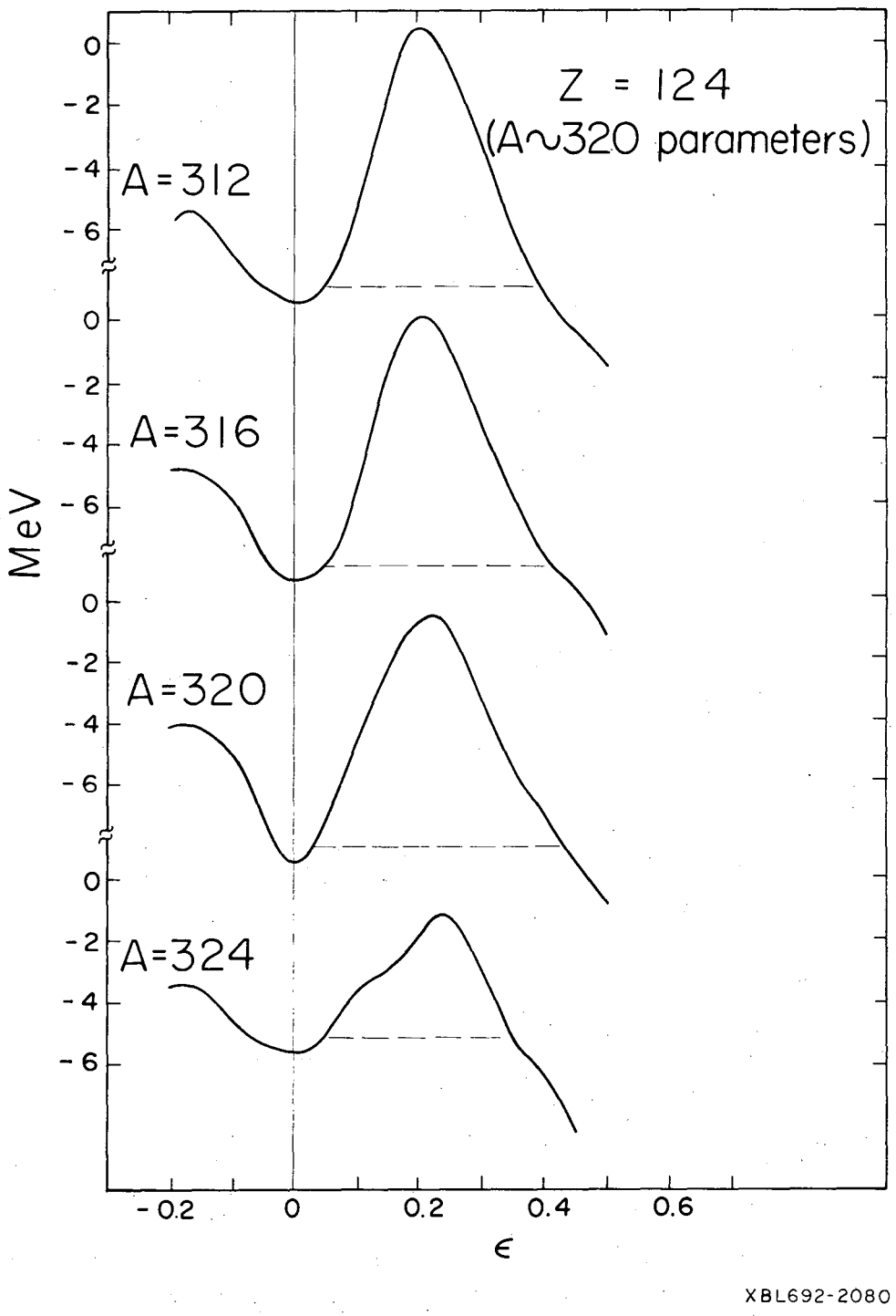
Z = 124
(A~320 parameters)
A=312
A=316
A=320
A=324
MeV
0
-2
-4
-6
-0.2
0
0.2
0.4
0.6
ϵ
XBL692-2080

Fig. 3j.

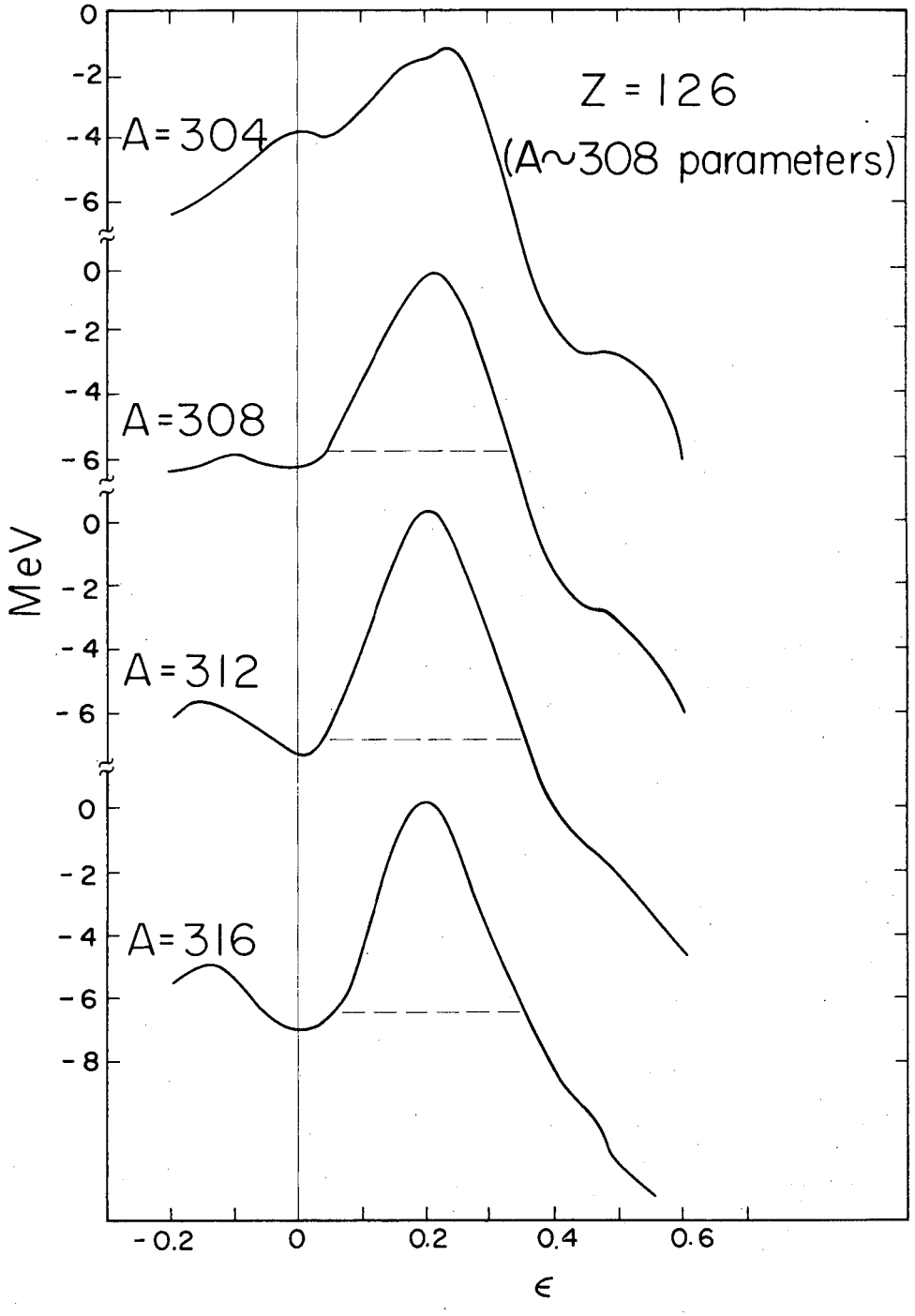
Z = 126
(A~308 parameters)
A=304
A=308
A=312
A=316
MeV
0
-2
-4
-6
-8
-0.2
0
0.2
0.4
0.6
ϵ
XBL692 - 2087

Fig. 3k.

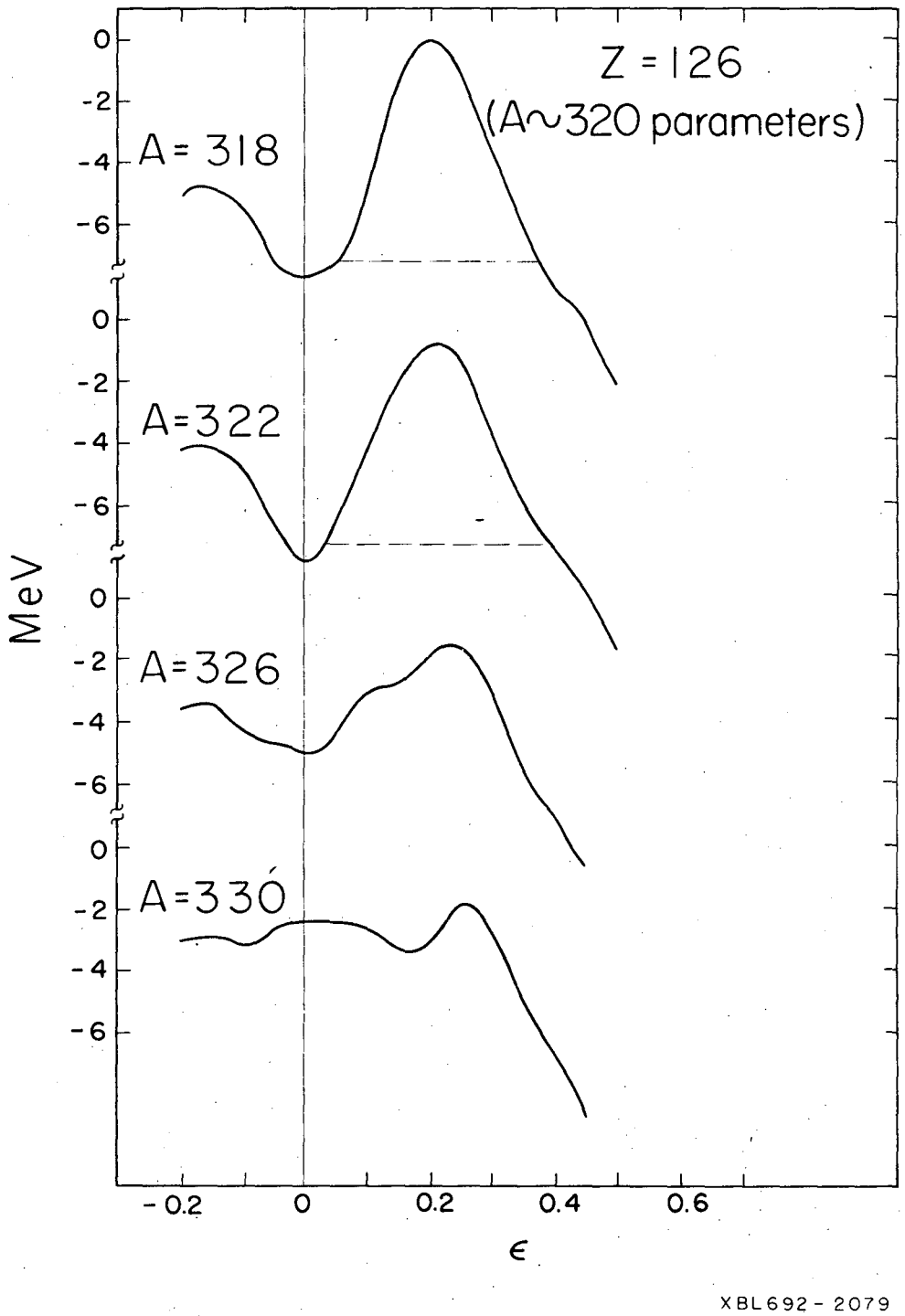
Z = 126
(A~320 parameters)
A = 318
A=322
A=326
A=330
MeV
0
-2
-4
-6
-0.2
0
0.2
0.4
0.6
ϵ
XBL692-2079

Fig. 3ℓ.

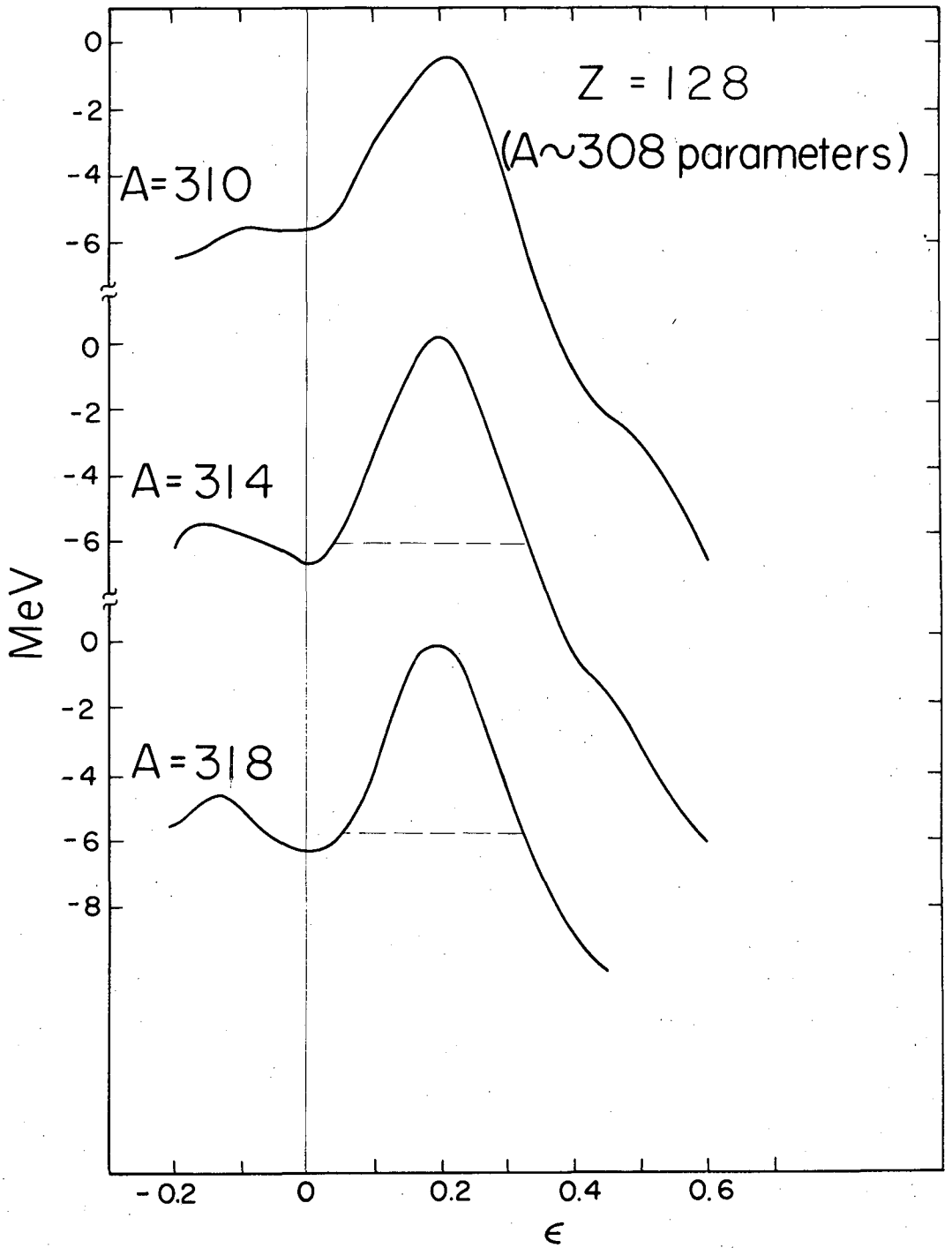
Z = 128
(A~308 parameters)
A=310
A=314
A=318
MeV
0
-2
-4
-6
-8
-0.2
0
0.2
0.4
0.6
ϵ
XBL692-2088

Fig. 3m.

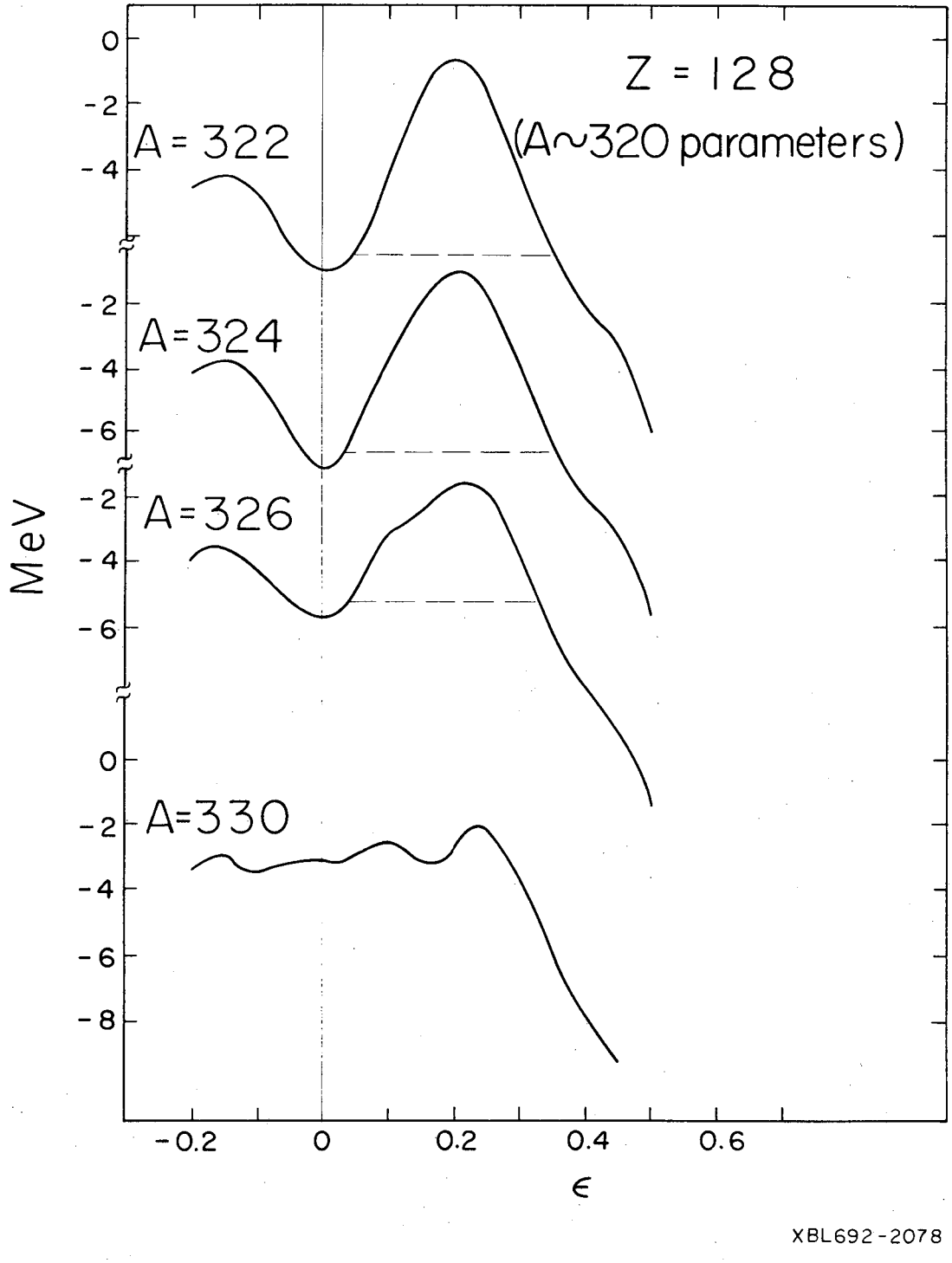
Z = 128
(A~320 parameters)
A = 322
A=324
A=326
A=330
MeV
0
-2
-4
-6
-8
-0.2
0
0.2
0.4
0.6
ϵ
XBL692-2078

Fig. 3n.

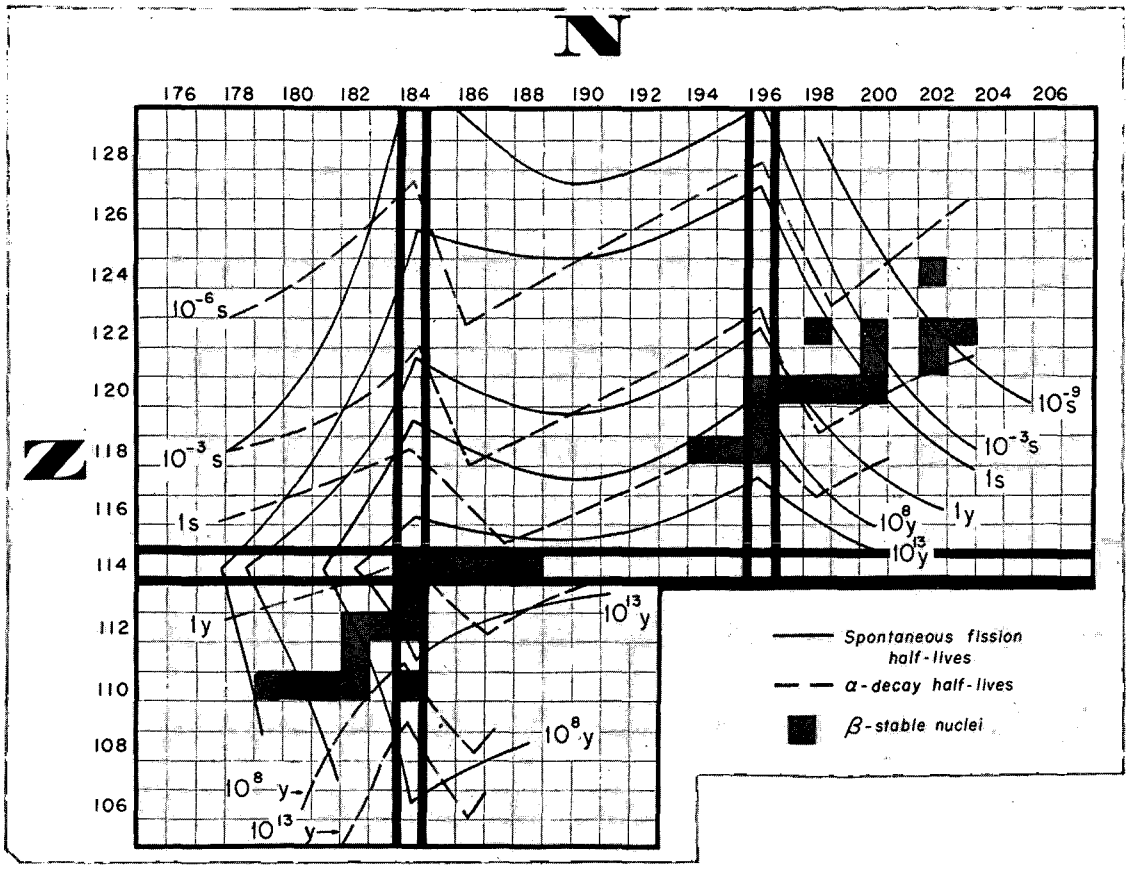

XBC 692-1535

Fig. 4

TECHNICAL INFORMATION DIVISION
LAWRENCE RADIATION LABORATORY
UNIVERSITY OF CALIFORNIA
BERKELEY, CALIFORNIA 94720